
Proceedings Paper:
Ai, S. and Long, H. orcid.org/0000-0003-1673-1193 (2022) Biaxial tension under bending and compression - development of a new formability test for incremental sheet forming. In: IOP Conference Series: Materials Science and Engineering. The 19th International Conference on Metal Forming (MF 2022), 11-14 Sep 2022, Online. IOP Publishing , 012066.

https://doi.org/10.1088/1757-899x/1270/1/012066

Biaxial tension under bending and compression - development of a new formability test for incremental sheet forming

To cite this article: S Ai and H Long 2022 *IOP Conf. Ser.: Mater. Sci. Eng.* **1270** 012066

Biaxial tension under bending and compression - development of a new formability test for incremental sheet forming

S Ai and H Long*
Department of Mechanical Engineering, the University of Sheffield, Sheffield, S1 3JD, UK
* Corresponding author, E-mail: h.long@sheffield.ac.uk

Abstract. A new testing method, Biaxial Tension under Bending and Compression (BTBC), is developed to investigate the effect of different deformation modes on material formability in Incremental Sheet Forming (ISF). A cruciform specimen is designed by simulating the material deformation under biaxial tension using Finite Element (FE) method. In the BTBC experimental testing, the cruciform specimen can be stretched in biaxial directions and the strain ratio of the two perpendicular directions can be varied. Furthermore, the superimposed effect of compression, bending and cyclic loading can be investigated. Material formability of aluminium alloy AA5251-H22 under plane strain path is tested. True strains of the specimen under different deformation modes are obtained by measuring distortions of circular grids inscribed onto the surface of the specimen. The experimental results show that the introduction of bending and compression contributes to localised material deformation. Material formability is improved by the introduction of bending, which is further enhanced by applying compression and cyclic loading. The BTBC test overcomes the limitation of commonly used testing methods in ISF formability studies, providing a fundamental explanation of the effect of strain path and loading conditions on the material deformation and fracture behaviour in ISF.

1. Introduction

Incremental sheet forming (ISF) has attracted extensive research interests and studies in the last decades due to its unique process flexibility and scalability for forming various geometrical shapes without the need of using customised dies and tools. A typical single point incremental forming (SPIF) only requires a set of clamping tools, a backing plate, one forming tool of a simple geometry. The forming tool moves along predesigned toolpaths and gradually deforms the clamped sheet metal into a desired shape and its movement can be controlled by a CNC machine. The material plastic deformation in SPIF is localised owing to the combined effect of tension, bending and shearing under cyclic tool movement, as shown in figure 1. However, the simple SPIF process compromises its potential industrial applications due to its relatively low forming accuracy resulted from springback after trimming thus its limitations in manufacturing complicated geometries [1-3].

To control springback, two basic methods were proposed to reduce stress gradient through thickness or introduce additional deformation to compensate for springback [4]. Based on these methods, double sided incremental forming (DSIF) was developed [5-6] by introducing a support tool to the forming tool as a partial die on the other side of the sheet metal, as shown in figure 2. The forming tool and supporting tool can be independently controlled and the relative position between the two tools can be adjusted. When the sheet is pressed between the forming and supporting tool, an additional compressive force is imposed. Therefore the material deformation in DSIF not only includes tension, bending and shearing but also compression under cyclic tool movements [7], as shown in figure 2. By developing a purposely designed DSIF machine [7], no backing plates were required for specific geometries in DSIF. In addition

to maintaining all the advantages of SPIF, DSIF improves forming accuracy as well as process flexibility when manufacturing complicated geometries.

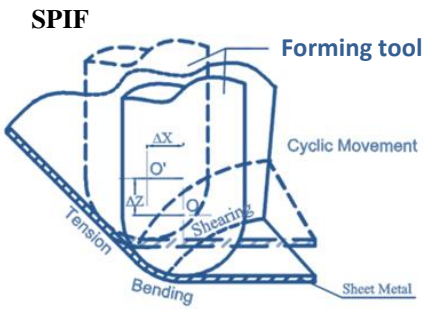

Figure 1. Deformation modes in SPIF.

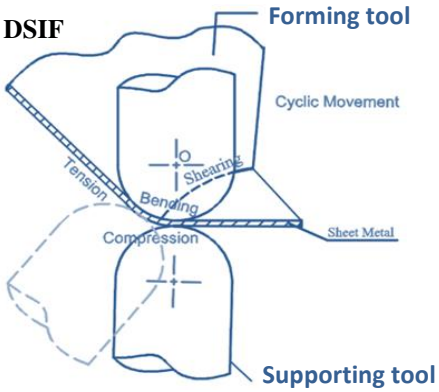

Figure 2. Deformation modes in DSIF.

2. Formability test methods in ISF

Material formability was significantly improved in ISF processes when compared with conventional sheet metal forming processes. For SPIF, its improved formability was attributed to the localised material deformation by a combination of tension, bending, shearing and cyclic loading [8-9]. For DSIF, the deployment of the supporting tool introduced an additional compressive loading onto the material, which further strengthened the localised deformation [7]. Regarding the deformation mechanism resulting in fracture occurrence in SPIF, it was suggested that the fracture of the material in SPIF might be an intrinsic property of the material and it followed the fracture forming limit (FFL) or forming limit of the material. Once the limit was met, fracture occurred. Based on the finite element (FE) analysis and experiments using AA1050-H111, it was concluded that the failure of the SPIF parts was better predicted by FFL curves rather than conventional forming limit curves (FLCs) [10]. As can be seen in figure 3, the FFLs of SPIF were very close to the FFL curves obtained from conventional fracture tests, especially near the plane strain path. For DSIF, the effect of the compression was not only determined by its magnitude but also the relative position of the forming and supporting tools, as illustrated in figure 2. Adjusting the relative position of the forming and supporting tools in DSIF simultaneously changed the division of the deformation zones, thus affecting the strain and stress distributions in the deforming zone of the sheet metal. Consequently, the forming limits were affected, as shown in figure 4.

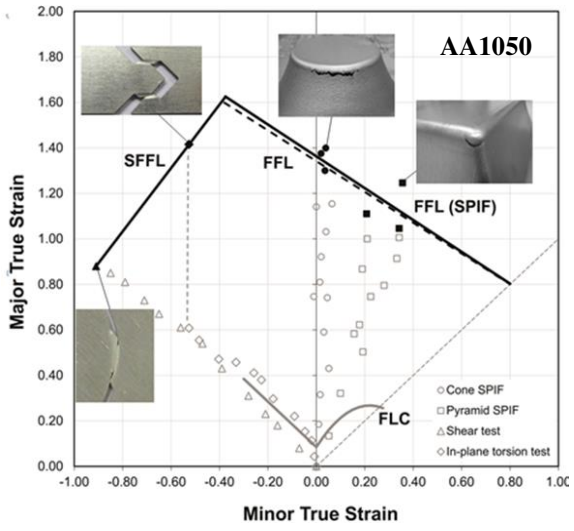

Figure 3. Fracture forming limits in SPIF [10].

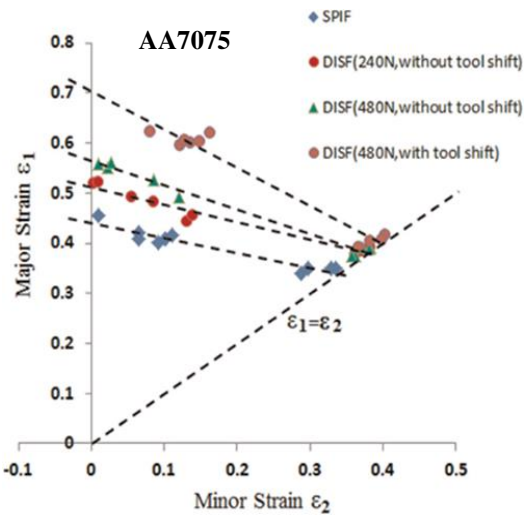

Figure 4. Forming limits in DSIF [7].

From the existing research, however, it is not clear that among tension, bending, shearing and compression effects, which one is the most dominant deformation mode affecting the material formability in ISF. According to the digital image correlation observation, different deformation modes dominated in SPIF when different process parameters were used. Bending effect was more dominant when the formed parts had a greater wall angle while through thickness shearing was more dominant for the parts with a smaller wall angle [9]. By varying process parameters including tool size, sheet thickness and wall angle in the FE simulation, the composition of the internal energy and the ratio between different energy components also changed, suggesting a shift of relative importance of the deformation modes [11].

Before the ISF development, the individual and combined effect of the deformation modes on material formability in conventional sheet metal forming processes has already been reported. The combined effect of bending and tension was investigated by developing a stretch-bending test [12] and a mathematical model [13]. It was shown that the introduction of bending into pure tension could lead to material formability improvement due to the reduced tensile effect caused by the compression effect on the concave side of the sheet in the thickness direction. However, it would not produce such a dramatic change of material formability enhancement as that observed in SPIF, compared with that predicted by the traditional FLCs. The contact stress between the tool and sheet metal could also lower the tensile stress needed for initiating material yielding thus strengthening the localised deformation resulted from bending effect. In the monotonic loading case, the existence of the localised deformation could eventually propagate to fracture since it created a weak spot in the material. However, in SPIF, the cyclic contact between the forming tool and sheet created a shift of the weakest spot, thus suppressing the development of damage in one spot thus resulting in significantly improved material formability [14]. This theory was proved by the Taraldsen test, in which copper material achieved a maximum uniform elongation of 600% [15] and mild steel material reached 590% [16].

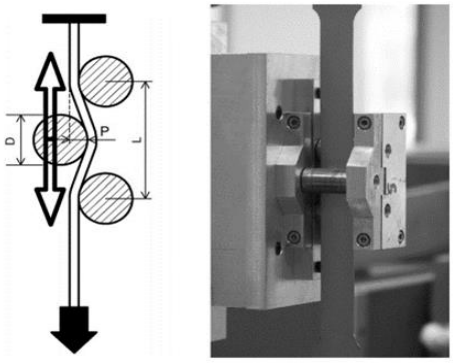

Figure 5. CBT test [18].

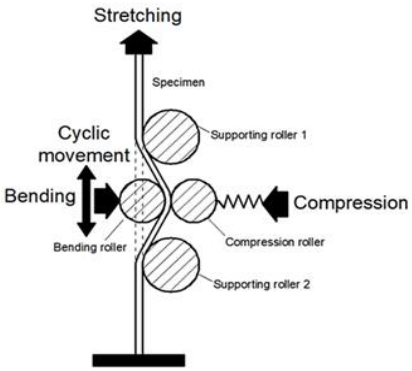

Figure 6. TCBC test [19].

However, the complicated loading and contact conditions between the tool and sheet prohibited a systematic and direct analysis of the factors affecting the material formability in ISF [14]. In addition, the introduction of compression effect further improved the material formability in DSIF. By performing the Nakazima tests, it was concluded that the bending effect itself could not explain the much delayed fracture in ISF [17]. The cyclic loading was another factor that contributed to the improved formability in ISF. However, to which degree the material formability could be enhanced and how it differed from the prediction made by the traditional testing methods remained unexplored. Recently, representative ISF tests were developed, including the continuous bending under tension (CBT) test for SPIF [18] and the tension under cyclic bending and compression (TCBC) test for both SPIF and DSIF [19]. In the CBT test, as shown in figure 5, the complicated contact conditions in ISF were simplified into a two-dimensional model. The tension, bending and cyclic effects were superimposed onto each other. Using the CBT test, localised deformation and reduced levels of tensile force to achieve the required plastic deformation were observed. In addition, multiple locations of necking were observed on the failed specimens. It was also observed that when the tensile speed was high enough, the CBT test was

degenerated to the simple tension test and the bending effect was less noticeable. In the TCBC test, as shown in figure 6, the major deformation modes in DSIF, including tension, bending, shearing and compression with cyclic loading effect, were independently controlled by adjusting corresponding testing parameters. It was found that among various deformation modes, the compression was the most significant factor affecting the material formability for AA5251-H22 and AA6082-T6 sheets tested [19]. Bending in general was beneficial to the material formability improvement, however its effect was influenced by the magnitude of compression loading applied. Localised material plastic deformation in the contact zone was further strengthened under the TCBC condition when an appropriate range of the compression was applied, reducing the tensile force required for initiating plastic deformation thus delaying the occurrence of fracture. However different materials showed different sensitivity to the variation of the test parameters [19].

Both the CBT and TCBC tests enabled investigations of the effect of the relevant deformation modes on the material formability in SPIF and DSIF processes. However, in the planer directions of the specimens in these tests, the material is under geometric constraint in only one direction, the longitudinal direction of the specimen. While in SPIF, it has been proved that the material is under a strain path between plane strain and equi-biaxial tension depending on the process parameters and geometry of the part being formed, as shown in figure 3. Different strain paths, such as uniaxial tension, plane strain and biaxial tension, show a major effect on the material deformation thus the material formability. Generally, a material can achieve a higher degree of deformation under biaxial tensile condition than it is under plane strain path in the conventional sheet metal forming processes [20]. The serrated strain path in SPIF was reported [17] and [21], and further confirmed by the FE simulation results of SPIF and DSIF process modelling [19]. The effect of strain paths on the material formability could not be reflected in the CBT and TCBC tests and the strain paths obtained from these tests were considerably different from those obtained from SPIF and DSIF processes. To overcome this limitation, the biaxial tension under bending and compression (BTBC) test is developed in this study and plane strain or biaxial tension, superimposed with bending and compression under cyclic loading can be investigated.

3. Development of the BTBC test method

3.1. Concept of the BTBC test

A schematic of the concept of BTBC testing is shown in figure 7. In the test, a cruciform specimen is stretched on all ends in both directions. By controlling the tensile speed, the strain ratio between the two perpendicular directions can be varied. The bending effect is provided by pushing a bending tool with a hemispherical head against the specimen to a certain bending depth. By changing the bending depth, the degree of the bending effect can be studied. On the other side of the specimen, a supporting tool is pushed against the specimen to provide a compression to the specimen. By controlling the supporting force of the tool, the compressive effect can be studied. The cyclic loading can be realised by controlling movement of the bending tool and applying the tensile force at a certain frequency. The bending tool can be lifted up from the specimen and the tensile force from the arms of the cruciform specimen can be released to remove the loadings. Furthermore, the bending can be reapplied by positioning the bending tool to the original depth, tension can be resumed by simply applying the tension again.

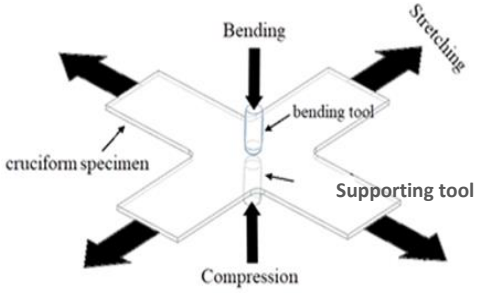

Figure 7. Schematic of the BTBC test.

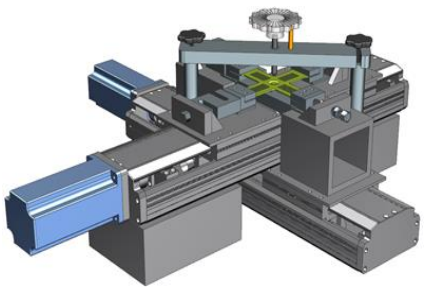

Figure 8. CAD model of the BTBC test.

3.2. Development of the BTBC test rig

Based on the proposed concept, the BTBC test rig is designed and manufactured. The rig comprises of two main components, the mechanical part and the electrical part. The mechanical part consists of structures designed to hold the specimen and to apply various loading conditions, and the CAD design is shown in figure 8. The electrical part is designed to control the motors. It consists of the power control box and the motor controlling system. Both parts are fixed onto a thick aluminium plate to maintain the stability, rigidity and integrity of the test rig, as shown in figure 9.

3.2.1. Application of biaxial tension. To simplify the positioning requirement of the motors and the clamps in order to guarantee that the centre of the cruciform specimen maintains its position throughout the test, two bidirectional linear screw sliders are used, as shown in figure 10. Different from traditional screw sliders, the effective length of the linear screw in each bidirectional linear screw slider is divided into two sections, the lead direction of the threads in one section is opposite to those in the other section. As a result, once the screw is motivated by the motor, the two carriages will move in the opposite directions simultaneously at the same speed.

As shown in figure 10, the two bidirectional linear screw sliders are positioned perpendicular to each other. The first slider is fixed onto the base directly while the second slider is positioned above the first one and they cross over in the middle point of the effective length of the sliders. Only two motors are needed, each motor is responsible for the movement of the slider in one planar direction. The bi-directional sliders can meet the requirement of positioning accuracy for the motors/sliders. As for the controlling system, the synchronisation of the motors in the opposite directions can also be avoided. Two servo motors (HML40-01030LI) are used to drive the sliders and each slider has a rated rotational speed of 3000 *rpm* and a constant rated output torque of 0.32 *Nm*. In order to obtain a lower speed range and a higher and stable output torque from the motor, a planetary gearbox (DS042-L2) with speed reduction ratio of 70:1 is coupled with each motor. As a result, the rated rotational speed of the servo motor-gearbox system is reduced to 43 *rpm* while the output torque applied onto the slider shaft is increased to 22.4 *Nm*.

The rotational speed of the servo motors can be varied by using the motor controllers and the movement of both motors can be started simultaneously with the help of the power control box, thus the effect of different strain paths can be investigated. In particular, if the motor in the transverse direction stays static and the motor in the longitudinal direction runs at a certain speed, the plane strain condition can be created. If both motors run at the same speed, it corresponds to the equi-biaxial tension condition.

3.2.2. Application of bending and compression. Bending is applied by the bending tool with a hemispherical head. Considering the dimension of the specimen and the commonly used forming tool size in the ISF processes, the diameter of the bending tool head is decided to be 10 *mm*, figure 7. As shown in figures 8 and 11, a beam structure is designed to hold the bending tool, pointing to the centre of the specimen. The beam is supported by two supporting pillars, which are fixed onto the base plate. Threads are cut onto the shank of the bending tool, by turning the bending tool clock-wisely, the tool will move downwards and it will push the centre of the specimen. The bending tool is attached to a plastic transparent wheel with marks inscribed. By counting the number of turns of the wheel, the downward distance of the bending tool can be calculated, thus the bending depth can be controlled.

Compression to the central area of the specimen is applied by the spring positioned on the other side of the sheet specimen, as shown in figure 11. The spring is housed in the spring holder, which is fixed onto the second slider. A steel cap is placed on top of the spring so that a surface contact between the specimen and the spring can be maintained. In order to guarantee that the specimen is in contact with the cap when springs with different lengths are used, caps with different thicknesses are manufactured. The thickness of the steel cap adopted in the test depends on the gap between the spring and the lower surface of the specimen. When the spring is compressed due to the downward movement of the bending tool, supporting force is generated. In addition, springs with different stiffness can be used in the test, so that the magnitude of the compressive force can be controlled without changing the bending depth, making the compression effect independent of the bending effect.

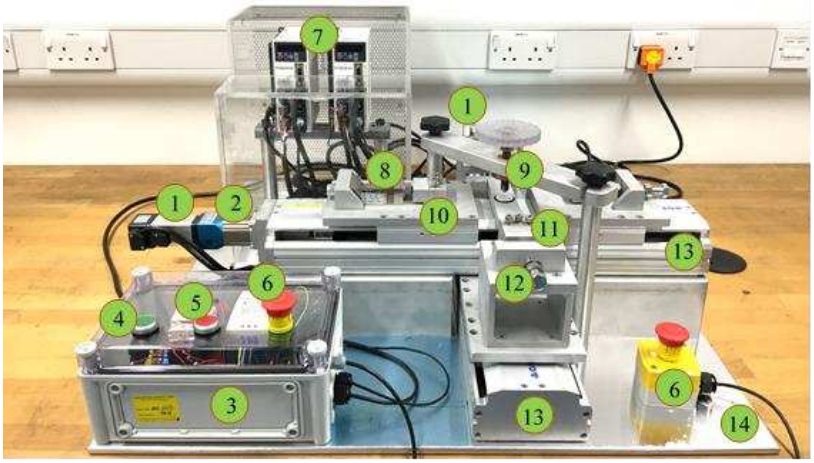

1. Motor; 2. Gearbox; 3. Power control box; 4. Power On button; 5. Power Off button; 6. Emergency Stop; 7. Motor controller; 8. Load cell; 9. Bending tool; 10. Spring; 11. Clamp; 12. Clamp position adjustment screw set; 13. Bidirectional linear screw; 14. Base plate

Figure 9. Full assembly of the BTBC test rig.

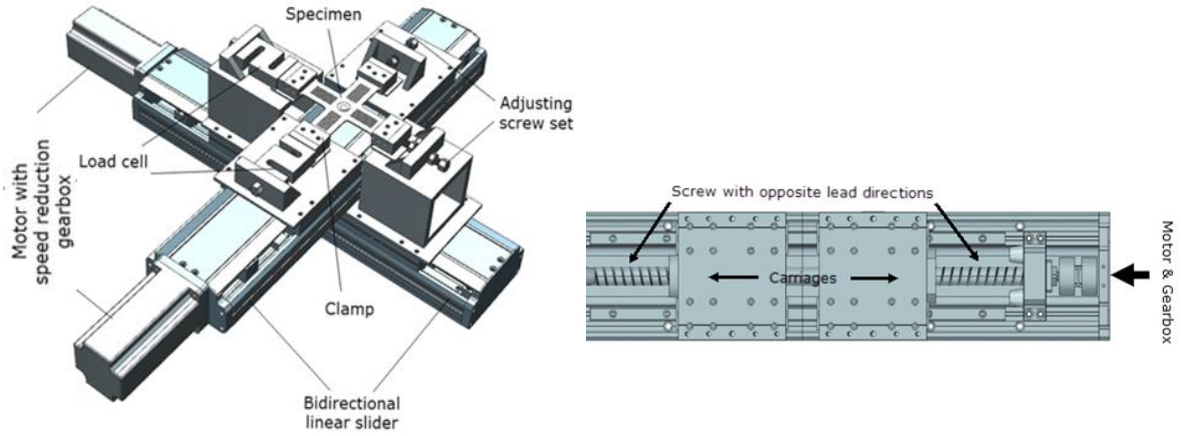

Figure 10. Biaxial tension loading components and bidirectional linear screw sliders.

4. Design optimisation of the cruciform specimen

The geometry of the cruciform specimen designed for biaxial tensile test should satisfy three conditions: cross shape, slots in the arms and tapered thickness in the centre of the specimen. Based on the geometries designed in [22-23] for thin metal sheets and taking the dimensions of the bidirectional sliders of the BTBC rig into consideration, an initial design of the cruciform specimen for material AA5251-H22 is proposed for the current study, as shown in figure 12. The original thickness of the sheet is 2 *mm* and the thickness of the central area is reduced to 0.75 *mm*. The diameter of the central area is 10 *mm*, matching the dimension of the bending tool. Slots with a length of 35 *mm* are created in the arms and the distance between the two bordering slots is 14 *mm*. As a result, only three design parameters are to be optimised for the geometry of the cruciform specimen, including the number of slots in each arm, the width of the arms, and the diameter of the central tapered area D in figure 12.

4.1. Finite element optimisation of the specimen geometry

In order to optimise the three design parameters, a FE model of the equi-biaxial tensile process is established by using the Abaqus/Explicit solver. As shown in figure 13, considering that the specimen is symmetric about both central planes and the loadings applied are also symmetrical, only a quarter of

the specimen is included in the FE model. Symmetric boundary conditions are applied onto the cross-sections of the specimen. The clamping area of the arms are defined to be rigid, while the rest of the specimen is deformable. The tensile speed of the clamps is equal to 1 *mm/min*. Solid element type C3D4 is used in the mesh of the specimen. Element size in the central zone and its neighbouring area is set to be 0.25 *mm*, while in the arms and clamping areas, it is set to be 2 *mm*. The flow stress data from the uniaxial tensile test of material AA5251-H22 is used to define the material plasticity in the FE model. By considering the maximum achievable equivalent plastic strain is around 0.15 in the uniaxial test and generally higher strains can be obtained in the biaxial test, it is decided in the optimization process the FE simulation is terminated when the maximum equivalent plastic strain of the elements reaches 0.2.
The variation of the values of the investigated parameters is selected based on the geometries designed in [22-23], as listed in figure 13. The arm width is firstly decided, then the radius of the central area, and finally the slot number is to be optimised. According to [22], in order to guarantee that the fracture occurs right in the centre of the specimen, the centre should be the thinnest. However in this study, the main purpose is to limit the maximum deformation to the central zone, not necessarily in the actual centre of the specimen. In order to achieve this, in the FE simulation, the objective of the optimisation is to find out the value of parameters that could produce the largest deformation in the central zone, rather than in the arms or in the slots.

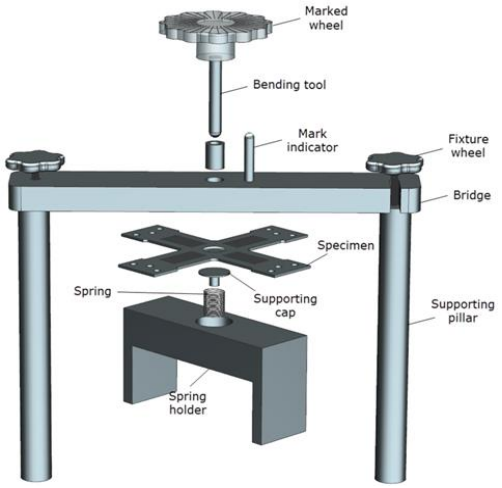

Figure 11. Bending/compression in the BTBC test.

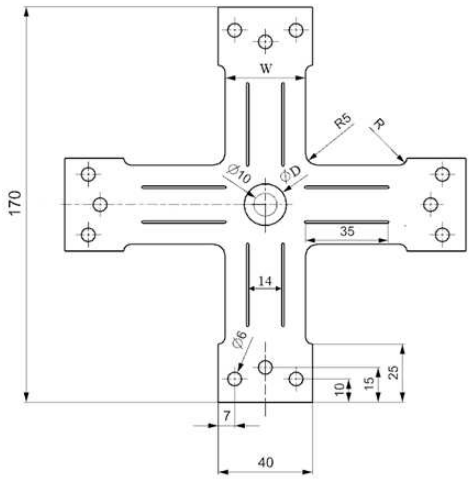

Figure 12. Initial design of the cruciform specimen.

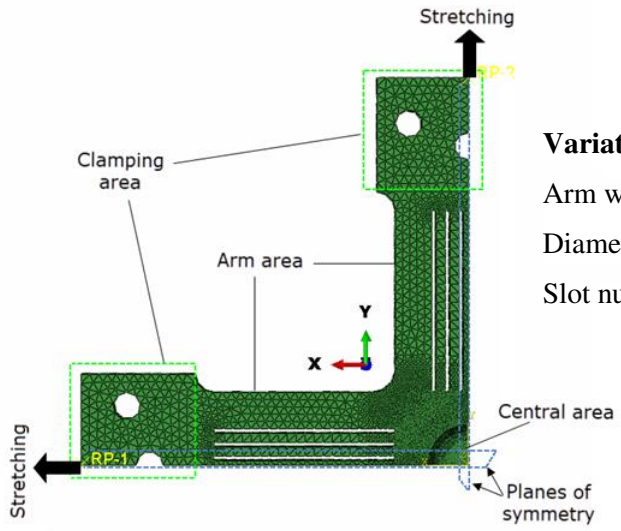

Variation of design parameters:

Arm width: 30, 32, 34 *mm*

Diameter of central tapered area: 18, 20 *mm*

Slot number: 3, 4, 5, 6

Figure 13. FE model of the cruciform specimen for geometry design optimisation.

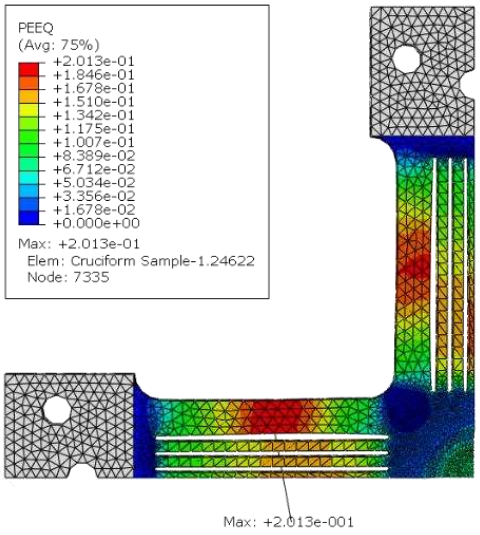

(a) Arm width 30 mm and 6 slots.

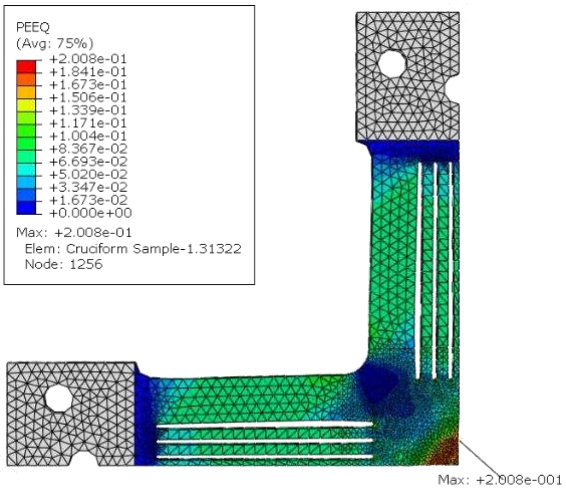

(b) Arm width 34 mm and 6 slots (optimised design).

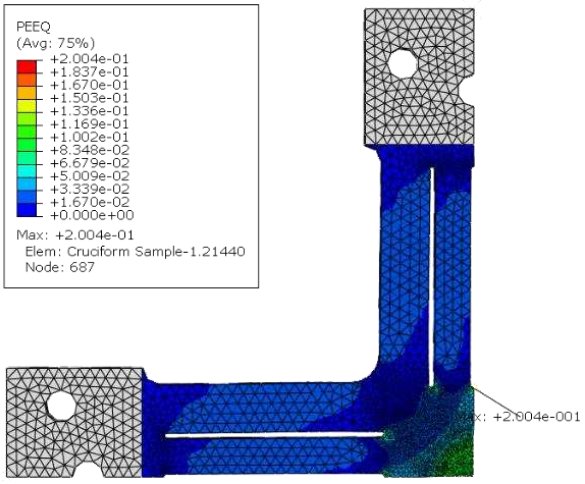

(c) Arm width 34 mm and 3 slots.

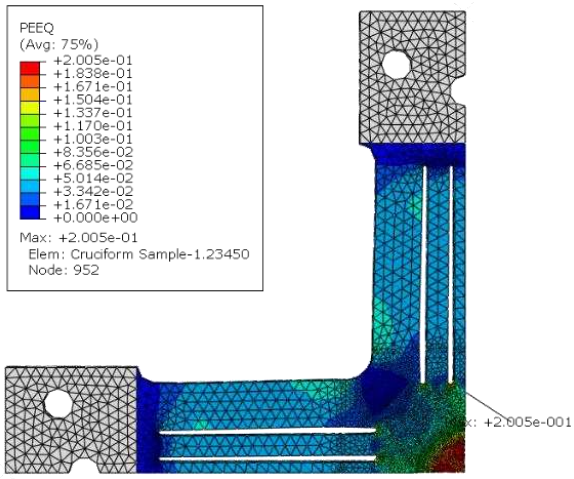

(d) Arm width 34 mm and 5 slots.

Figure 14. Equivalent plastic strain distributions of the specimen using different design parameters.

4.2. Results of finite element optimization of the specimen geometry

The optimisation process of the arm width is firstly performed and the strain distribution in the specimen using different arm widths is obtained when the largest equivalent plastic deformation of the element reaches around 0.2. The location of the element with the largest deformation is marked out in the results. In the first FE model, the diameter of the central tapered area D is set to be 18 *mm*, and three slots are cut in each arm.

The results of the equivalent plastic distribution are selected from some of the FE models and these are shown in figure 14. As can be seen, when the arm width is 30 *mm*, the largest plastic deformation occurs in the arm and an obvious distortion is observed, which indicates the fracture would first occur in the arms. While when the arm width is 32 *mm*, the largest deformation appears at the end of the slot. When it is increased to 34 *mm*, the largest deformation occurs in the central area. As a result, the arm width is determined to be 34 *mm*. When the diameter of the central tapered area D is increased from 18 to 20 *mm*, the largest plastic deformation occurs in the transition area between the arm and the central area. By comparison, plastic deformation is more concentrated in the central tapered area D when the diameter is 18 *mm*. As a result, the diameter of the central tapered area used in the specimen is 18 *mm*.

The deformed specimens with a slot number of 3, 4, 5 and 6 are compared. As shown in figure 14, fewer slots in the arms create lower strains in the arms. The arm area in the specimen with 3 slots undergoes the least degree of deformation while the one with 6 slots is under the highest deformation in the arms. However, only the specimen with 6 slots produces the highest plastic deformation in the central area, while for the rest, the highest deformation all occurred at the tips of the slots. As a result, the number of slots in the arm is selected to be 6.

5. Experimental tests and results under plane strain condition

5.1. Design of experimental tests

In this paper, the material deformation under plane strain path is presented. As shown in table 1, five sets of tests are performed and in each test the specimen is under different loading condition, including: 1- plane strain; 2- plane strain with bending; 3- plane strain with cyclic bending; 4- plane strain with bending and compression; 5- plane strain with cyclic bending and compression. For each loading condition, three or four repeated tests are performed.

The motor speed is set to be 35 *rpm*, creating a moderate tensile speed of the 2.5 *mm/min* by the slider, adopted from the biaxial tensile test in [23]. In the TCBC test [19], the bending depth of 6 *mm* and compressive force of 900 *N* produced an obvious improvement of material formability for the material AA5251-H22. Considering that the bending tool head has a diameter of 10 *mm* in the BTBC test, the dual contact area between the tool, the supporting plate and the specimen should be a fraction of that in the TCBC test. Assuming that the radius of the contact area is 1 mm, the area of the contact zone should be about 1/6 of that in the TCBC test. As a result, in order to maintain a similar level of stress to that in the TCBC test, the bending depth is set to be 7 *mm* in the BTBC test. The stiffness of the spring used in the test is 23.4 *N/mm*, resulting in a supporting force of 163.8 *N*.

Table 1. Design of BTBC experimental tests under plane strain condition

Test No.	Plane strain	Bending	Compression	Cyclic loading
1	✓	-	-	-
2	✓	✓	-	-
3	✓	✓	-	✓
4	✓	✓	✓	-
5	✓	✓	✓	✓

Cyclic loading of tension, bending and compression onto the specimen is manually controlled. In the ISF tests, the tool radius of 5-10 *mm* is commonly used while the vertical step per revolution about the central axis of the cone shape is 0.1-1 *mm*, which makes that the number of contact between the tool and the sheet is around 10 when the tool incrementally deforms the same region of the material. As a result, the unloading/loading process is performed 10 times in each test where cyclic loading is required to be applied. The time gap between each unloading/loading process is 1/10 of the total time of the pure plane strain tests before the fracture of the specimen. After 10 cycles of loading, the specimen is continuously deformed with the loadings until fracture occurs. The unloading of the bending effect is made by lifting up the bending tool until the contact between the tool and the specimen is removed. The unloading of tension is applied by reversing the motor rotation with a small angle so that the clamps are moved back and the tensile force is decreased to a minimal value.

5.2. Experimental of results of plastic strain at fracture

In order to obtain the strain distribution on the surface of the specimen after each test, grid pattern is inscribed onto the surface of the specimen with laser marking. The grid consists of circles of a diameter of 1 *mm*, and the pattern covers a central area of 10×10 *mm*. After deformation, a perfect circular shape

is distorted into an elliptical shape. By measuring dimensions of the ellipse in the major and minor axes by using a portable microscope, and comparing those with the circle radius, the true strain in each direction could be calculated. In order to obtain the maximum plastic strain of the material achieved before fracture, the radii of the deformed circles close to the cracks of the specimen are measured.

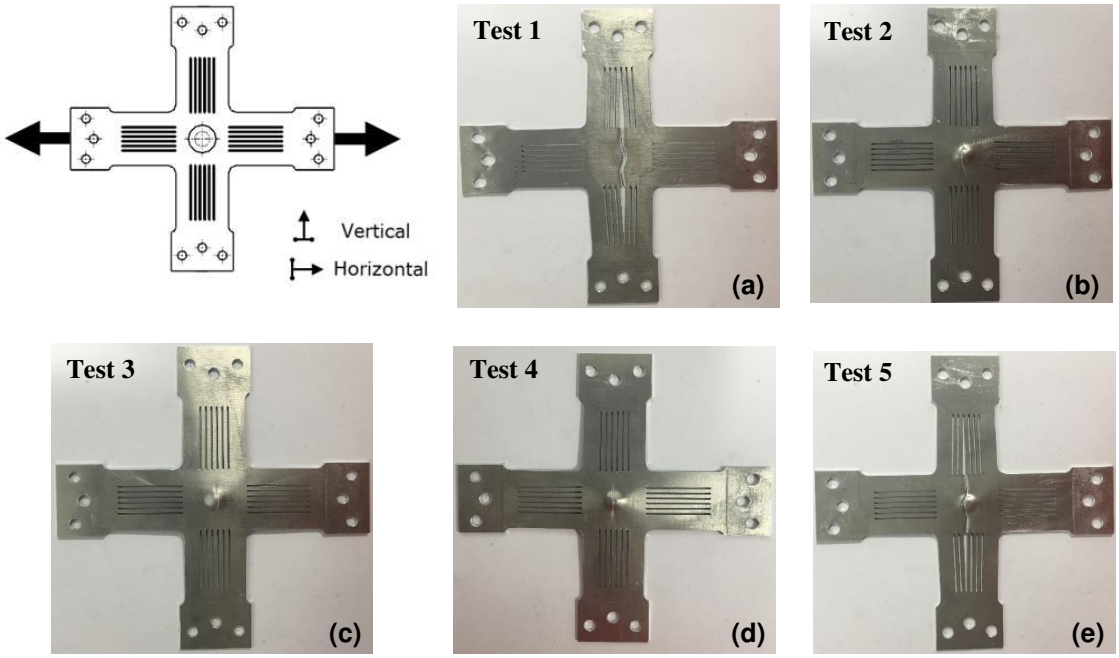

Figure 15. Specimens after deformation under plane strain path with different loading conditions: Test 1: plane strain; Test 2: plane strain with bending; Test 3: plane strain with cyclic bending; Test 4: plane strain with bending & compression; Test 5: plane strain with cyclic bending & compression.

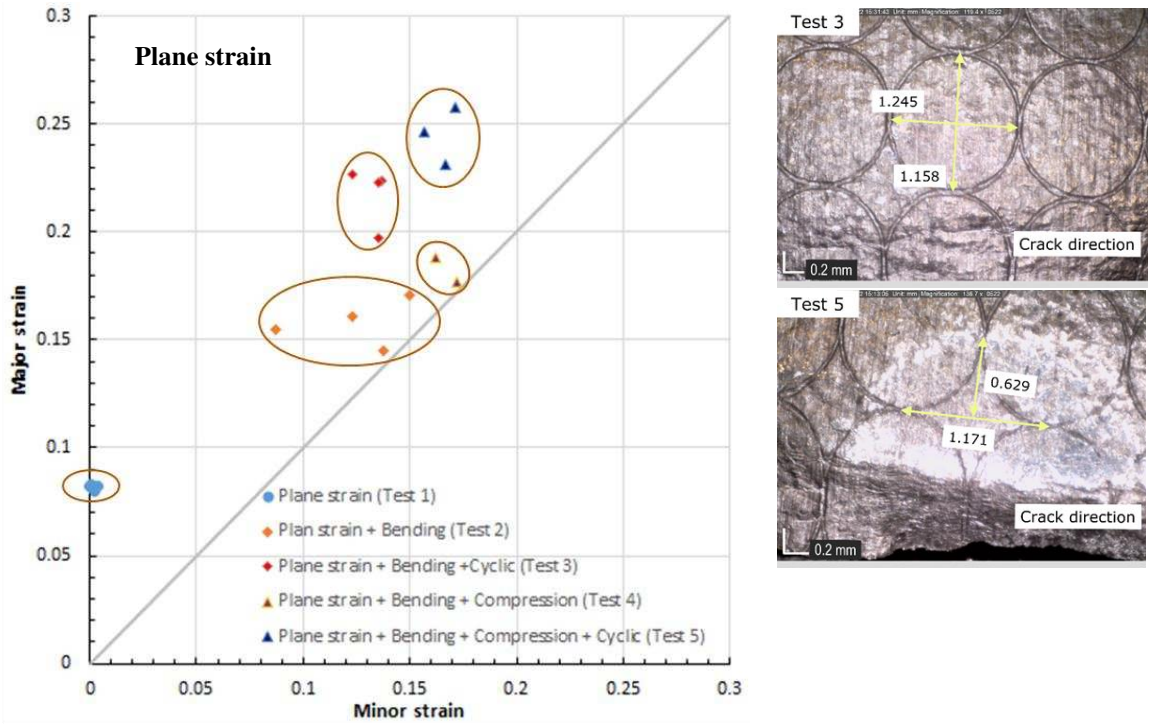

Figure 16. Formability improvement under plane strain with various loading conditions.

Under the plane strain path with different loading conditions, fractured specimens in Tests 1-5 are shown in figure 15. The relative position of the specimen in relation to the stretching direction is illustrated by the schematic. For the pure plane strain condition, the fracture occurs abruptly and a huge crack appears across the central area of the specimen, as shown in figure 15(a). While with additional loadings applied, the cracks are largely constrained to the centre of the specimen, as shown in figure 15 (b), (c), (d) and (e). In addition, the orientation of all cracks is perpendicular to the stretching direction, suggesting that the tension applied contributes to the occurrence of fracture in all the tests.

The radii of the deformed circles near the cracks are measured by using the microscope. True strains in the two directions are calculated according to the measurement of the radii of the deformed circles, and they are plotted in the major strain - minor strain space in order to compare the material formability between different tests. As shown in figure 16, compared with the condition of pure plane strain when only the tension applied (Test 1), the other four tests all show much higher forming limits before fracture when subjected to more complicated loading conditions. Among these four conditions, generally, material forming limits under tension and bending conditions show the lowest forming limit (Test 2), followed by tension, bending and compression (Test 4), then tension, bending and cyclic loading (Test 3). Material shows the highest formability under tension, bending, compression and cyclic loading (Test 5). In addition, comparing Test 2 and Test 4, it is clear that material formability is slightly enhanced when compression is superimposed onto tension and bending. By comparing Test 2 and Test 3, Test 4 and Test 5, respectively, it is clear that the major strain in the tensile direction is increased significantly from roughly 0.15 to 0.19 and 0.16 to 0.22 respectively when cyclic loading is introduced. It indicates that the cyclic loading could improve the material forming limit considerably.

The loading conditions change the plastic deformation history of the material in the tests. As can be seen in figure 16, the distribution of the points in the major strain - minor strain space can be categorised into two regions. In Test 1, the points are all close to the pure plane strain condition, while in the other four tests, the points are closer to equi-biaxial tension condition. The difference is caused by the bending effect. In the tests, bending is applied by the bending tool with a hemispherical head. While bending is being applied and the arms of the specimen are clamped, consequently the geometrical constraints lead to biaxial deformation in the central area. However, when comparing Test 2 and Test 3, it is clear that the increased strain only happens in the major strain direction (the tensile direction). The same trend can also be observed for the Test 4 and 5, suggesting the formability improvement in the tests under plane strain condition.

6. Conclusions

A new testing method, the biaxial tension under bending and compression (BTBC) test, is developed in this study to investigate the effect of strain path on the material formability enhancement under various deformation conditions presented in ISF processes. Based on the results obtained from experimental testing, the following conclusions can be made:

- Under plane strain, the tested material AA5251-H22 shows varied deformation behaviours under different loading conditions.
- The application of additional bending improves the material formability, which is further improved by the superimposition of compression.
- When cyclic loading of the bending and compression is superimposed onto the tension, the material formability could be further enhanced.
- The BTBC test could be used as a simplified method to investigate the material deformation in the SPIF and DSIF processes.

References

[1] Bambach, M., Araghi B T and Hirt G 2009 *Production Engineering* **3(2)** pp 145-156
[2] Duflou J R, Habraken A M, Cao J, Malhotra R, Bambach M, Adams D, Vanhove H, Mohammadi A and Jeswiet J 2018. *International journal of material forming* **11** pp 743-773

[3] Gerhard H, Kordtomeikel R, Bremen T, Laugwitz M and Bailly D 2021 *Forming the Future, Proc. Int. Conf. on Technology of Plasticity (Ohio)* (USA, the Minerals, Metals & Materials Series) **1** pp 507-521
[4] Micari, F, Ambrogio G and Filice L 2007 *Journal of Materials Processing Technology* **191(1)** pp 390-395
[5] Meier H, Magnus C, Smukala V 2011 *CIRP Annals Manufacturing Technology* **60(1)** pp 327-330
[6] Maidagan E, Zettler J, Bambach M, Rodríguez P and Hirt G 2007 *Key Engineering Materials* **344** pp 607-614
[7] Lu B, Fang Y, Xu DK, Chen J, Ai S, Long H, Ou H and Cao J 2015 *International Journal of Machine Tools & Manufacture* **93** pp 37-48
[8] Emmens W and Van den Boogaard A 2009 *Journal of Materials Processing Technology* **209(8)** pp 3688-3695
[9] Eyckens P, Belkassem B, Henrard C, Gu J, Sol H, Habraken AM, Duflou J R, Van Bael A and Van Houtte P 2011 *International journal of material forming* **4(1)** pp 55-71
[10] Silva MB, Skjoedt M, Bay N and Martins PAF 2009 *The Journal of Strain Analysis for Engineering Design* **44(4)** pp 221-234
[11] Maqbool F and Bambach M 2018 *International Journal of Mechanical Sciences* 136 pp 279-292
[12] Demeri MY (1981). *Journal of Applied Metalworking* **2(1)** pp 3-10
[13] El-Domiaty AA, Shabara MAN and Al-Ansary MD 1996 *International Journal of Advanced Manufacturing Technology* 12(3) pp 207-220
[14] Ai S and Long H 2019 *International journal of Advanced Manufacturing Technology* **104** pp 33–61
[15] Taraldsen A 1964 *Material Testing* **6(6)** pp 189-228
[16] Rosochowski A and Olejnik L 1988 *International journal of mechanical sciences* **30(1)** pp 51-60
[17] Centeno G, Bagudanch I, Martínez-Donairea AJ, García-Romeub ML, and Vallellanoa C 2014 *Materials & Design* **63** pp 20-29
[18] Emmens W and Van den Boogaard A 2009 *Journal of Materials Processing Technology* **209(14)** pp 5456-5463
[19] Ai S, Dai R and Long H 2020 *Journal of Materials Processing Technology* **275**, 116349
[20] Embury J and Duncan J 1981 *Annual Review of Materials Science* **11(1)** pp 505-521
[21] Eyckens P, He S, Van Bael A, Van Houtte P and Duflou J 2007 *AIP Conference Proceedings* **908** pp 141-146
[22] Song X 2018. Identification of forming limits of sheet metals with an in-plane biaxial tensile test *INSA de Rennes.* p 175
[23] Shao Z, Li N, Lin J and Dean TA 2016 *Experimental Mechanics* **56(9)** pp 1489-1500

Acknowledgments
The authors wish to acknowledge the funding support received from the UK EPSRC through project grant EP/T005254/1. The authors would also like to thank Jamie Booth, David Webster and Gareth Barker of the mechanical workshop, Michael Herbert and Chris Todd of the electronics workshop of the Department of Mechanical Engineering for their assistance in the development of the biaxial tension under bending and compression (BTBC) test rig.